research papers

X-ray four-quadrant diamond phase-retarder system to compensate for off-axis and chromatic aberrations

Kouhei Okitsu,[a]* Yoshinori Ueji,[b] Kiminori Sato[b] and Yoshiyuki Amemiya[b,c]

[a]Engineering Research Institute, The University of Tokyo, Yayoi, Bunkyo, Tokyo 113-8656, Japan, [b]Department of Applied Physics, The University of Tokyo, Hongo, Bunkyo, Tokyo 113-8656, Japan, and [c]Department of Advanced Materials Science, The University of Tokyo, Hongo, Bunkyo, Tokyo 113-8656, Japan. Correspondence e-mail: okitsu@soyak.t.u-tokyo.ac.jp

An X-ray transmission-type double phase-retarder system that can compensate for off-axis aberration (phase-shift inhomogeneity due to angular divergence of incident X-rays) has been developed and its advantage over a conventional single transmission-type X-ray phase retarder was demonstrated. However, it was noticed that the transmission-type X-ray phase retarder suffers from not only off-axis aberration but also chromatic aberration (phase-shift inhomogeneity due to energy spread of incident X-rays). In this paper, a transmission-type X-ray four-quadrant phase-retarder system is proposed that can compensate for both off-axis and chromatic aberrations. The X-ray four-quadrant phase-retarder system is composed of four transmission-type X-ray phase retarders. The scattering planes of four phase-retarder diamond crystals are set to be inclined by $45°$, $135° (= 45° + 90°)$, $225° (= 45° + 180°)$ and $315° (= 45° + 270°)$, respectively, with respect to the plane of incident polarization. Under the conditions of 7709 eV photon energy, 1.5 eV energy spread and $45''$ angular divergence (FWHM) of incident X-rays, the X-ray four-quadrant phase-retarder system created 0.98 degree of vertical-linear polarization from horizontal-linear polarization. This value was favorably compared to 0.89 and 0.96, which were obtained by the single and double phase-retarder systems, respectively. The principle of the X-ray four-quadrant phase-retarder system will be described together with its advantage over the single and double phase-retarder systems.

1. Introduction

The feasibility of an X-ray phase retarder utilizing diffractive birefringence in a perfect crystal was pointed out by Skalicky & Malgrange (1972) for the first time. From that time on, in cooperation with the advent of synchrotron radiation, several candidates of reflection-type phase retarder using X-rays reflected by perfect crystals were suggested by Hart (1978), Annaka *et al.* (1980), Annaka (1982), Golovchenko *et al.* (1986) and Mills (1987), but did not reach general practical use. In this period, Hart & Rodrigues (1979) developed an energy-tunable X-ray polarizer and analyzer working with an extremely high extinction ratio (σ-polarization:π-polarization reflectivity ratio $>10^4$).

Transmission-type X-ray phase retarders were developed by Hirano, Ishikawa, Kikuta and their co-workers (Hirano *et al.*, 1991; Ishikawa *et al.*, 1991; Hirano *et al.*, 1992; Ishikawa *et al.*, 1992; Hirano *et al.*, 1993, 1995; Hirano, 1996) and Giles and his co-workers (Giles, Malgran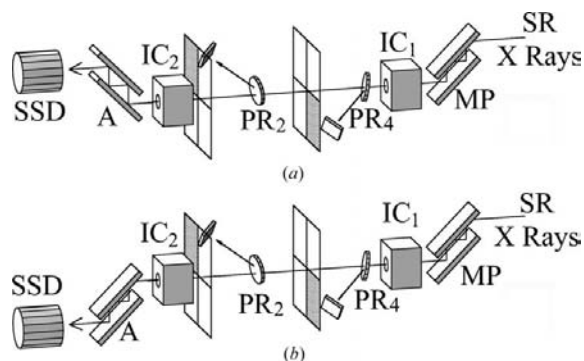ge, Goulon, Vettier *et al.*, 1994; Giles, Malgrange, Goulon, Bergevin *et al.*, 1994; Giles *et al.*, 1995), in which an X-ray wave transmitted through a diffracting perfect crystal in the vicinity of the Bragg condition was used as output. This has been recognized nowadays as a decisive X-ray phase retarder. While both reflection- and transmission-type X-ray phase retarders utilize phase shifts between σ- and π-polarized X-rays in a diffracting perfect crystal, Hirano and his co-workers noticed that the phase shift between σ and π polarizations of transmitted X-rays was more insensitive to the X-ray incident angle on a crystal compared to that of reflected X-rays. In spite of this advantage of the transmission-type phase retarder, collimation of incident X-rays is necessary when a strictly defined polarization state is demanded, as pointed out by Hirano *et al.* (1993). In other words, the transmission-type phase retarder still suffers from phase-shift inhomogeneity owing to angular divergence of incident X-rays (off-axis aberration).

In order to overcome this problem of the transmission-type X-ray phase retarder, we proposed an X-ray double phase-

retarder system to compensate for off-axis aberration and demonstrated its advantage over the single phase retarder (Okitsu *et al.*, 2001).

An X-ray polarization switching technique was developed by using the X-ray double phase-retarder system. This technique was successfully applied to the imaging of polarization contrasts arising from X-ray natural linear dichroism (XNLD) (Sato, Okitsu *et al.*, 2000; Sato, Ueji *et al.*, 2000), magnetic circular dichroism (XMCD) (Sato, Ueji *et al.*, 2000; Sato, Ueji, Okitsu, Matsushita & Amemiya, 2001; Sato, Ueji, Okitsu, Matsushita, Saito *et al.*, 2001*a*) and magnetic linear dichroism (XMLD) (Sato, Ueji, Okitsu, Matsushita, Saito *et al.*, 2001*b*). Also, spectra of natural circular dichroism (XNCD) (Ueji *et al.*, 2000) were measured. XNCD spectra were measured by Goulon *et al.* (1998) and Alagna *et al.* (1998) for the first time by using a helical undulator which generates circularly polarized synchrotron radiation at ESRF. In contrast with their method, our measurement of XNCD spectra was performed by using the circular-polarization switching technique with the X-ray double phase retarders in combination with horizontal-linearly polarized synchrotron X-rays from a normal bending magnet.

The X-ray double phase retarders that compensate for off-axis aberration can create high degrees of polarization even with divergent incident X-rays. However, the estimation of X-ray double phase retarders reported in our previous article (Okitsu *et al.*, 2001) did not take into account chromatic aberration, *i.e.* phase-shift inhomogeneity due to an energy spread of incident X-rays. In this paper, (i) experiments to show the chromatic aberration of the X-ray double phase retarders in §2, (ii) principle of X-ray four-quadrant phase-

retarder system to compensate for both off-axis and chromatic aberrations in §3 and then (iii) experiments that reveal the advantage of the four-quadrant phase-retarder system over the double and single phase retarder(s) in §4 and §5 will be described.

2. Chromatic aberration of the transmission-type X-ray phase retarder

In our previous paper (Okitsu *et al.*, 2001), we compared the double phase retarders and the single phase retarder with regard to the off-axis aberration. The double phase retarders created 0.99° of vertical-linear polarization from horizontal-linear polarization while the single phase retarder of the same total thickness created 0.87°. This experiment was performed near the Ni *K*-absorption edge (8333 eV) with the experimental arrangement shown in Fig. 1(*a*). In this case, the energy spread of X-rays outgoing from the analyzer crystal was estimated to be 0.07 eV from a consideration using the DuMond diagram (DuMond, 1937).

Recently, we have performed similar experiments near the Co *K*-absorption edge (7709 eV) with experimental arrangements shown in Figs. 1(*a*) and 1(*b*) in order to investigate the effect of the energy spread of incident X-rays on the X-ray phase retarder. From a consideration using the DuMond diagram, the energy spread of an X-ray wave outgoing from
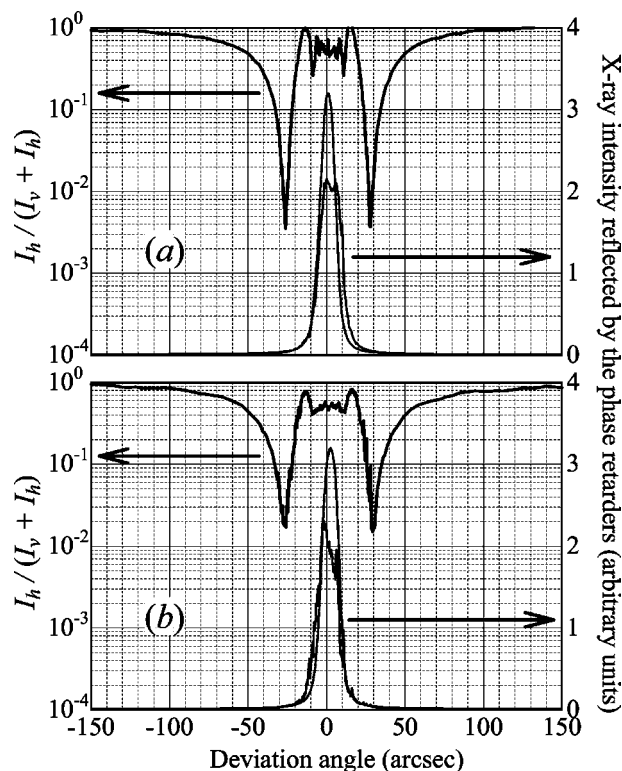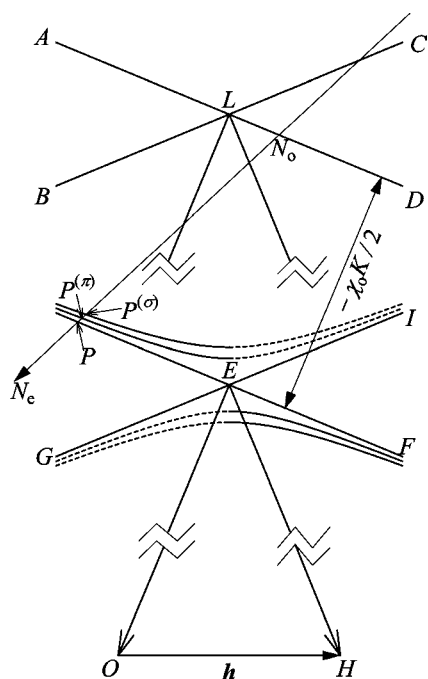

Figure 1
The double (two-quadrant) X-ray phase-retarder system placed between Hart–Rodrigues's (Hart & Rodrigues, 1979) Si 422 polarizer and analyzer. (*a*) The polarizer and analyzer were arranged in (+ − +−, − + −+) antiparallel Nicol geometry. Then the energy range is 0.09 eV. (*b*) The polarizer and analyzer were arranged in (+ − +−, + − +−) parallel Nicol geometry. The energy spread was 0.5 eV. MP: a silicon channel-cut monochromating polarizer equipped with Hart–Rodrigues's offset mechanism (Hart & Rodrigues, 1979) giving four-bounced 422 reflection in a symmetric Bragg geometry. A: an analyzer crystal similar to the polarizer. PR$_2$ and PR$_4$: diamond (100)-oriented phase-retarder crystals giving 111 reflection in an asymmetric Laue geometry whose thicknesses are 314 and 313 μm, respectively. IC$_1$ and IC$_2$: ionization chambers. SSD: a solid-state detector of germanium. Reflected X-rays from the two diamond phase retarders are monitored by two PIN photodiodes.

Figure 2
Rate of a residual horizontally polarized component of X-rays measured by rotating the two phase retarders simultaneously. (*a*) was measured under the setup shown in Fig. 1(*a*) with an energy spread of X-rays of 0.09 eV. (*b*) was measured under the setup shown in Fig. 1(*b*) with an energy spread of X-rays of 0.5 eV.

the analyzer crystal is estimated to be 0.09 eV for Fig. 1(*a*) and 0.5 eV for Fig. 1(*b*). Figs. 2(*a*) and 2(*b*) show experimental results under the setups shown in Figs. 1(*a*) and 1(*b*), respectively. The abscissas are angular deviations of the phase retarders, $\Delta\theta$. The right ordinates in arbitrary linear scales are X-ray intensities reflected by the two phase-retarder crystals. The left ordinates in logarithmic scales are $I_h/(I_v + I_h)$, where I_v and I_h are vertically and horizontally polarized components of X-ray intensity incident on the analyzer crystal, respectively. Values of $I_h/(I_v + I_h)$ were calculated from X-ray intensities measured with IC_2 and SSD based on the procedure described in our previous paper (Okitsu *et al.*, 2001). The degree of vertical-linear polarization, P_v, is defined as follows:

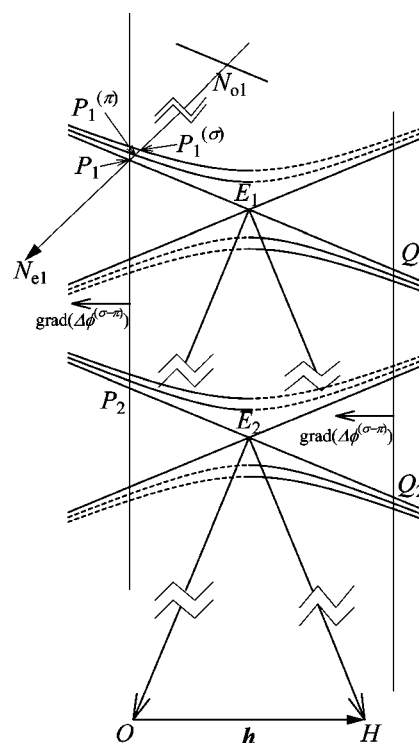$$P_v \equiv \frac{I_v - I_h}{I_v + I_h} = 1 - \frac{2I_h}{I_v + I_h}. \quad (1)$$

The maximum degrees of vertical-linear polarization, $P_v^{(L.\text{max})}$ and $P_v^{(R.\text{max})}$, were obtained at angular positions of left and right dips shown in Fig. 2. $P_v^{(L.\text{max})}$ and $P_v^{(R.\text{max})}$ were 0.993 in the case of Fig. 2(*a*). On the other hand, they were 0.966–0.970 in the case of Fig. 2(*b*). Thus, the maximum degrees of vertical polarization created with the double X-ray phase retarders deteriorate when the energy spread becomes wider. This phenomenon is attributed to chromatic aberration, *i.e.* phase-shift inhomogeneity due to an energy spread of incident X-rays.

3. Principle of a four-quadrant X-ray phase-retarder system to compensate for both off-axis and chromatic aberrations

Fig. 3 shows dispersion surfaces for σ and π polarizations of a phase-retarder crystal. The dispersion surfaces for π polarization are closer to asymptotes *PF* and *GI* by a factor of $\cos 2\theta_B$ than those for σ polarization, where θ_B is the Bragg angle of the phase-retarder crystal. *E* at which asymptotes *PF* and *GI* cross is the Lorentz point. Lines *AD* and *BC* are loci of distance *K* from the origin *O* of the reciprocal space and a reciprocal-lattice point *H*, respectively. *K* is $1/\lambda$, where λ is the wavelength of incident X-rays in an atmospheric path. *L* at which *AD* and *BC* cross is the Laue point. Distances between lines *AD* and *PF* and between lines *BC* and *GI* are $-\chi_o K/2$, where χ_o is the zeroth-order Fourier component of electric susceptibility of the phase-retarder crystal. According to the dynamical diffraction theory, when X-rays are incident on a perfect crystal with an angle lower than the Bragg condition, tie points on upper branches of dispersion surfaces are dominant for transmitted X-rays in Fig. 3, whereas those on lower branches are mainly excited with an incident angle higher than the Bragg condition. Thus, dominant and less dominant parts of dispersion surfaces with regard to transmitted X-rays are drawn by solid and dashed curves, respectively, in Fig. 3 (and in Fig. 4). When an X-ray beam with a wave-number vector of $\overrightarrow{N_oO}$ is incident on a phase-retarder

Figure 3
Important and less important parts of dispersion surfaces regarding σ–π phase shift of transmitted X-rays are drawn by solid and broken curves, respectively. *L*: Laue point, *E*: Lorentz point. Vector $\overrightarrow{N_oN_e}$ is normal to the crystal surface. The position of N_o is determined by angular deviation of the incident X-rays from the Bragg condition.

Figure 4
Two sets of dispersion surfaces corresponding to wavelengths λ (upper) and $\lambda + \Delta\lambda$ (lower). When X-rays with a wavelength of λ and a wave number vector of $\overrightarrow{N_{o1}O}$ are incident on a phase-retarder crystal, a vector $\overrightarrow{N_{o1}N_{e1}}$ normal to the surfaces of the crystal stimulates tie points $P_1^{(\sigma)}$ and $P_1^{(\pi)}$ on the dispersion surfaces, resulting in the phase-shift value $\Delta\phi^{(\sigma-\pi)}$ due to dispersion-surface gap $P_1^{(\sigma)}P_1^{(\pi)}$.

crystal whose surfaces are normal to vector $\overrightarrow{N_o N_e}$, tie points $P^{(\sigma)}$ and $P^{(\pi)}$ for σ and π polarizations are mainly excited. Now let us introduce a value of the phase shift $\Delta\phi^{(\sigma-\pi)} = \phi^{(\sigma)} - \phi^{(\pi)}$. Here, $\phi^{(\sigma)}$ and $\phi^{(\pi)}$ are phase advances given to σ- and π-polarized transmitted X-ray beams, respectively, by a phase-retarder crystal with respect to an atmospheric path. (An exact definition of advance and/or retardation of phase will be discussed later.) The $\sigma-\pi$ phase shift $\Delta\phi^{(\sigma-\pi)}$ is approximately given by the dispersion-surface gap $P^{(\sigma)}P^{(\pi)}$. As $\Delta\phi^{(\sigma-\pi)}$ depends on position N_o which is the initial point of the wave-number vector of the incident X-ray wave, this value can be regarded as a scalar function of point N_o. For simplicity, however, we regard $\Delta\phi^{(\sigma-\pi)}$ as a scalar function of position P in Fig. 3. When the wavelength is changed with a phase-retarder crystal fixed in real space, points N_o and P move simultaneously in the direction of vector $\overrightarrow{EO}$. On the other hand, when the incident angle is changed, these points move in the direction of vector $\overrightarrow{EF}$.

Fig. 4 shows dispersion surfaces with wavelengths λ and $\lambda + \Delta\lambda$, where $\Delta\lambda$ is a positive differential value of wavelength. When the wavelength changes from λ to $\lambda + \Delta\lambda$ in Fig. 4, changes of $\sigma-\pi$ dispersion-surface gaps are negligibly small since $\Delta\lambda$ is assumed to be sufficiently small. Consequently, dispersion surfaces surrounding Lorentz point E_2 with a wavelength of $\lambda + \Delta\lambda$ can be considered to shift just slightly from those surrounding Lorentz point E_1. Therefore, loci of constant values of $\Delta\phi^{(\sigma-\pi)}$ turn out to be contour planes whose cross sections are P_1P_2 and/or Q_1Q_2 perpendicular to the reflection vector $\mathbf{h}$ in Fig. 4. Consequently, the phase-shift gradient $\mathrm{grad}(\Delta\phi^{(\sigma-\pi)})$ is a vector normal to the contour plane P_1P_2 or Q_1Q_2. Here, let us consider the sign of $\mathrm{grad}(\Delta\phi^{(\sigma-\pi)})$. With regard to the dispersion surfaces drawn by solid curves at upper left of the Lorentz points E_1 and E_2, the phase of σ polarization is retarded and the absolute value of the retardation becomes smaller with tie points being farther from the Bragg condition. In this case, $\mathrm{grad}(\Delta\phi^{(\sigma-\pi)})$ is directed to the left. Based on a similar consideration for the solid curves lower right of the Lorentz points E_1 and E_2, the direction of $\mathrm{grad}(\Delta\phi^{(\sigma-\pi)})$ is the same as in the case of upper left dispersion surfaces. Since the phase-shift-gradient vector has

components parallel ($\overrightarrow{E_2O}$) and perpendicular ($\overrightarrow{E_2Q_2}$) to the direction of a wave-number vector of transmitted X-rays as shown in Fig. 4, the single and double transmission-type phase retarder(s) suffers from both off-axis and chromatic aberrations. The X-ray double phase retarders (Okitsu et al., 2001) can compensate for the off-axis aberration but still suffer from the chromatic aberration.

Fig. 5 shows the principle of a four-quadrant phase-retarder system that can compensate for both the off-axis and chromatic aberrations. The transmitted X-ray wave propagates from the right to the left. In parts (Q_1), (Q_2), (Q_3) and (Q_4) of Fig. 5, dispersion surfaces corresponding to phase retarders giving reflections in the directions of the first, second, third and fourth quadrants are shown, respectively, when viewed from the downstream direction. In the right part of Fig. 5, two orthogonal coordinate systems composed of unit vectors $\mathbf{e}_x, \mathbf{e}_y, \mathbf{e}_z$ and $\mathbf{x}, \mathbf{y}, \mathbf{z}$ are drawn. Here, $\mathbf{x} = (\mathbf{e}_x - \mathbf{e}_y)/2^{1/2}$, $\mathbf{y} = (\mathbf{e}_x + \mathbf{e}_y)/2^{1/2}$ and $\mathbf{z} = \mathbf{e}_z$. The incident X-rays are polarized in the direction of $\mathbf{e}_x$. The planes of incidence of the first-, second-, third- and fourth-quadrant transmission-type phase retarders are inclined with respect to the unit vector $\mathbf{e}_x$ by $45°$, $135° (= 45° + 90°)$, $225° (= 45° + 180°)$ and $315° (= 45° + 270°)$, respectively. In the cases of the first- and third-quadrant phase retarders, directions of σ and π polarizations of a transmitted X-ray wave are $\mathbf{x}$ and $\mathbf{y}$, respectively. On the contrary, in the cases of the second- and fourth-quadrant phase retarders, directions of σ and π polarizations of X-ray transmission are $\mathbf{y}$ and $\mathbf{x}$, respectively. This reversal of polarizations between odd-numbered-quadrant and even-numbered-quadrant phase retarders is the most critical point for compensation for chromatic aberration.

Now, let us define a small phase-shift value $\Delta\phi_n^{(L)}$ $(0 < \Delta\phi_n^{(L)} < \pi)$ which produces 'left-screwed' elliptical polarization whose electric vector rotates counterclockwise when viewed from the downstream direction, with nth-quadrant phase retarder ($n \in \{1, 2, 3, 4\}$). We have to consider what state of polarization the left-screwed polarization is. First, let us consider a couple consisting of a left-screwed bolt and a left-screwed nut whereas normal bolts and nuts are usually right-screwed. A left-screwed bolt can be regarded as a left-screwed polarization whose electric vector draws a left-screwed spiral when the time is stopped. A left-screwed nut is convenient for considering whether the polarity of rotation of an electric vector is clockwise or counterclockwise when the time is progressed or the position in the direction of wave propagation is changed. A pair of left-screwed bolt and nut is always left-screwed regardless of direction of view. The circumstances are the same even in the case of a right-screwed bolt and nut. In this way, to define the polarity of rotating polarization, we can avoid the confusion that the direction of view is from downstream or upstream of the wave propagation when
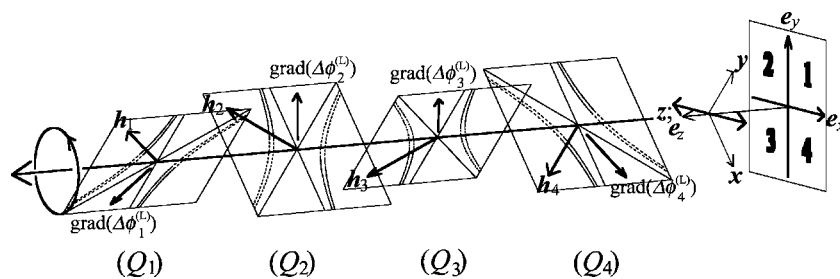

Figure 5
Principle of compensation for both off-axis and chromatic aberrations of a transmission-type X-ray phase retarder by using a four-quadrant phase-retarder system. In parts (Q_1), (Q_2), (Q_3) and (Q_4), dispersion surfaces corresponding to phase retarders giving reflections in the directions of the first, second, third and fourth quadrants, respectively, viewed from the downstream direction, are drawn. Numbers of quadrants are indicated for clarity. This three-dimensional figure is clarified in Fig. 6.

considering whether the rotation of the electric vector is clockwise or counterclockwise. Now, let us define a unit vector **z** which is directed downstream of the wave propagation and parallel to the bolt axis. Next, we define unit vectors **x** and **y** so that **x**, **y** and **z** construct a right-hand orthogonal coordinate system (see the right part of Fig. 5). When a left-screwed bolt moves without rotation in the direction of $+z$ with progress in time, a left-screwed nut whose position is fixed at a constant value of z rotates counterclockwise when viewed from $+z$ (viewed from the downstream direction of wave propagation) and clockwise when viewed from $-z$. Now, let us represent a wave field $\mathbf{D}(t, z) = \mathbf{x}D_x(t, z) + \mathbf{y}D_y(t, z)$ as follows:

$$\begin{pmatrix} D_x \\ D_y \end{pmatrix} = \begin{pmatrix} \mathrm{Re}\{D_x^{(o)} \exp[2\pi i(\nu t - k_x z)]\} \\ \mathrm{Re}\{D_y^{(o)} \exp[2\pi i(\nu t - k_y z)]\} \end{pmatrix}. \qquad (2)$$

Here, $D_x^{(o)}$ and $D_y^{(o)}$ are complex amplitudes at $t = 0$ and $z = 0$, but let us regard these values as plus real values for simplicity. ν is a plus frequency and k_x and k_y are plus wave numbers of x- and y-polarized waves, respectively. $\mathrm{Re}\{\eta\}$ is a real component of a complex value η. When $D_x^{(o)}$ and $D_y^{(o)}$ have the same amplitude and no phase difference, we can define a real value $D^{(o)}$, where $D^{(o)} = D_x^{(o)} = D_y^{(o)}$. In this case where the X-rays are horizontal-linearly polarized at $z = 0$, (2) is represented as follows:

$$\begin{pmatrix} D_x \\ D_y \end{pmatrix} = \begin{pmatrix} D^{(o)} \cos[2\pi(\nu t - k_x z)] \\ D^{(o)} \cos[2\pi(\nu t - k_y z)] \end{pmatrix}. \qquad (3)$$

When scalar values k_x and k_y are different and $\Delta\phi^{(x-y)} = 2\pi(k_y - k_x)z$, (3) is represented as follows:

$$\begin{pmatrix} D_x \\ D_y \end{pmatrix} = \begin{pmatrix} D^{(o)} \cos[2\pi(\nu t - k_x z)] \\ D^{(o)} \cos[2\pi(\nu t - k_x z) - \Delta\phi^{(x-y)}] \end{pmatrix}. \qquad (4)$$

Here, $\Delta\phi^{(x-y)} = \Delta\phi^{(x)} - \Delta\phi^{(y)}$, where $\Delta\phi^{(x)}$ and $\Delta\phi^{(y)}$ are phase advances given to x and y polarizations by propagation by a distance z in a (diffractive) birefringent material. In (4), $\Delta\phi^{(x-y)}$ is a value of phase retardation of y polarization, *i.e.* a value of phase advance of x polarization when phase advance is attributed to progress in plus time t. When $\Delta\phi^{(x-y)} = \pi/2$, (4) is represented as follows:

$$\begin{pmatrix} D_x \\ D_y \end{pmatrix} = \begin{pmatrix} D^{(o)} \cos[2\pi(\nu t - k_x z)] \\ D^{(o)} \cos[2\pi(\nu t - k_x z) - \pi/2] \end{pmatrix} \qquad (5)$$

$$= \begin{pmatrix} D^{(o)} \cos[2\pi(\nu t - k_x z)] \\ D^{(o)} \sin[2\pi(\nu t - k_x z)] \end{pmatrix}. \qquad (6)$$

The polarization state (D_x, D_y) represented by (6) is nothing but a left-screwed circular polarization, that is a polarization state whose electric vector rotates counterclockwise when viewed from $+z$ (downstream direction). Therefore, when the phase-shift value $\Delta\phi^{(x-y)} [= 2\pi(k_y - k_z)z]$ is $0 < \Delta\phi^{(x-y)} < \pi$, $\Delta\phi^{(x-y)}$ is a value that transforms the incident wave polarized in the direction of $\mathbf{x} + \mathbf{y}$ into a left-screwed polarization. Thus, when an $\mathbf{x}, \mathbf{y}, \mathbf{z}$ coordinate system is defined as shown in the right part of Fig. 5 and the incident beam is linearly polarized in the direction of $\mathbf{x} + \mathbf{y}$, $\Delta\phi_n^{(L)}$, which produces a left-screwed polarization, turns out to be

$$\Delta\phi_n^{(L)} = \phi_n^{(x)} - \phi_n^{(y)},$$
$$\text{where } n \in \{1, 2, 3, 4\}. \qquad (7)$$

As shown in Fig. 5, σ- and π-polarization states are contrary between $n \in \{1, 3\}$ and $n \in \{2, 4\}$. For a positive value of $\Delta\phi_n^{(L)}$, a phase of y polarization has to be retarded. Therefore, when $n \in \{1, 3\}$, $\Delta\phi_n^{(L)}$ are given by

$$\Delta\phi_n^{(L)} = \phi_n^{(\sigma)} - \phi_n^{(\pi)} = \Delta\phi_n^{(\sigma-\pi)},$$
$$\text{where } n \in \{1, 3\}. \qquad (8)$$

On the contrary, when $n \in \{2, 4\}$,

$$\Delta\phi_n^{(L)} = \phi_n^{(\pi)} - \phi_n^{(\sigma)} = -\Delta\phi_n^{(\sigma-\pi)},$$
$$\text{where } n \in \{2, 4\}. \qquad (9)$$

Here, $\phi_n^{(x)}$, $\phi_n^{(y)}$, $\phi_n^{(\sigma)}$ and $\phi_n^{(\pi)}$ are phase advances of x-, y-, σ- and π-polarized transmitted X-rays given by the nth-quadrant phase retarder with respect to an atmospheric path. It can be understood from Fig. 5 that directions of chromatic aberrations due to odd-numbered-quadrant and even-numbered-quadrant phase retarders are contrary and then cancelled out with each other.
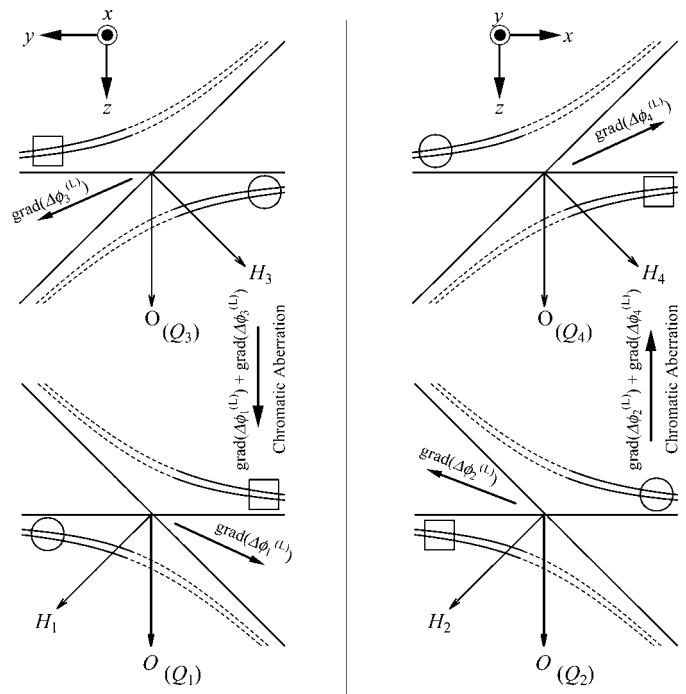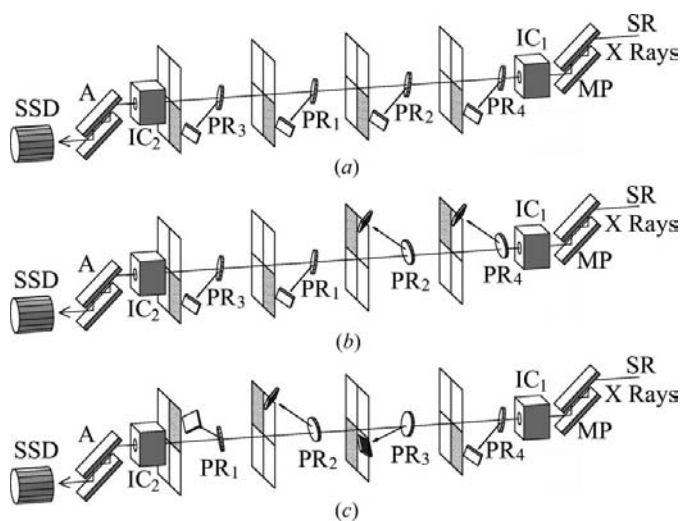

Figure 6
Four dispersion surfaces of a four-quadrant phase-retarder system. These figures clarify the three-dimensional Fig. 5 by drawing dispersion surfaces of odd-numbered-quadrant phase retarders on the left and those of even-numbered-quadrant phase retarders on the right. Suffix n ($n \in \{1, 2, 3, 4\}$) in Q_n, H_n and $\Delta\phi_n^{(L)}$ corresponds to an nth-quadrant phase retarder. The planes of the drawings are rotated by $90°$ around the direction of vector $\mathbf{z}$ (direction of transmitted X-ray propagation) between left- and right-hand drawings. It can be understood that directions of chromatic aberrations due to odd-numbered-quadrant and even-numbered-quadrant phase retarders are contrary and then cancelled out with each other. A left-screwed polarization ($\pi > \sum_{n=1}^4 \phi_n^{(L)} > 0$) is generated by using angular regions indicated by four circles. On the other hand, a right-screwed polarization ($0 > \sum_{n=1}^4 \phi_n^{(L)} > -\pi$) is generated at regions indicated by four squares.

forcelb > These circumstances are clarified in Fig. 6, in which dispersion surfaces of odd-numbered-quadrant phase retarders in the left part and those of even-numbered-quadrant phase retarders in the right part, are drawn, respectively. Fig. 6 shows that $\mathrm{grad}(\Delta\phi_1^{(L)}) + \mathrm{grad}(\Delta\phi_3^{(L)})$ are directed to the downstream direction of the transmitted X-rays, while $\mathrm{grad}(\Delta\phi_2^{(L)}) + \mathrm{grad}(\Delta\phi_4^{(L)})$ are directed to the upstream direction. Therefore, chromatic aberration due to the first- and third-quadrant phase retarders and that due to the second- and fourth-quadrant phase retarders are cancelled out by each other. A condition in which $\sum_{n=1}^{4} \mathrm{grad}(\Delta\phi_n^{(L)}) = 0$ can be realized by controlling the four-quadrant X-ray phase-retarder system so that absolute values of vectors $\mathrm{grad}(\Delta\phi_n^{(L)})$ are identical.

4. Experimental arrangement to evaluate the four-quadrant X-ray phase-retarder system

In order to evaluate the effect to compensate for the off-axis and chromatic aberrations with the four-quadrant X-ray phase-retarder system, we performed experiments, the arrangements of which are shown in Fig. 7. Experimental arrangements shown in Figs. 7(a), 7(b) and 7(c) are identical except for arrangements of four phase-retarder diamond crystals and photodiodes monitoring X-rays reflected by the four diamond crystals. Phase-retarder diamond crystals giving 111 reflection in an asymmetric Laue geometry were set in the following three kinds of geometries in Figs. 7(a), 7(b) and 7(c).

Figure 7
Experimental arrangements of quadruple phase retarders in (a) single (one-quadrant), (b) double (two-quadrant) and (c) four-quadrant geometries. MP: a silicon channel-cut monochromatizing-polarizer equipped with Hart–Rodrigues's offset mechanism giving four-bounced 422 reflection in a symmetric Bragg geometry. A: an analyzer crystal similar to the polarizer. PR_1, PR_2, PR_3 and PR_4: diamond (100)-oriented phase-retarder crystals giving 111 reflection in an asymmetric Laue geometry whose thicknesses are 318, 314, 301 and 313 μm, respectively. IC_1 and IC_2: ionization chambers. SSD: a solid-state detector of germanium. Reflected X-rays from the four phase retarders are monitored by four PIN photodiodes.

(i) All four diamond crystals gave reflections in the fourth-quadrant direction [Fig. 7(a); one-quadrant geometry].

(ii) PR_2 and PR_4 gave reflections in the second-quadrant direction and PR_1 and PR_3 gave reflections in the fourth-quadrant direction [Fig. 7(b); two-quadrant geometry].

(iii). PR_n ($n \in \{1, 2, 3, 4\}$) gave reflections in the nth-quadrant direction [Fig. 7(c); four-quadrant geometry].

Synchrotron white X-rays at the experimental station BL-4A of the Photon Factory, Institute of Materials Structure Science, were monochromated into 7709 eV (the Co K-absorption edge) and simultaneously horizontally polarized with a silicon channel-cut monochromatizing polarizer (MP) giving four-bounced 422 reflections in symmetric Bragg geometries. The monochromatizing polarizer was water-cooled and equipped with a Hart–Rodrigues off-set mechanism (Hart & Rodrigues, 1979). An angular offset of about $0.6''$ was applied between two sides of the channel. Owing to a Bragg angle ($46.5015°$) approximately equal to $45°$ and the offset mechanism, the extinction ratio of the polarizer (σ-polarization:π-polarization reflectivity ratio) was estimated to be $>10^7$ based on a calculation from the dynamical diffraction theory. This value was confirmed in a separate experiment. The analyzer (A) was a silicon crystal similar to the monochromatizing polarizer except for not being water-cooled. Planes of incidence of the polarizer and analyzer were adjusted to be parallel within an error of $0.1°$. The size of the X-ray beam was 2.5 mm (horizontal) $\times$ 2.0 mm (vertical). The horizontal angular divergence of incident X-rays was about $45''$ (FWHM). The energy spread of X-rays four-bounced-reflected by the monochromatizing polarizer was estimated to be 1.5 eV from the vertical beam size (2.0 mm) and the distance from the source (10 m). Since the polarizer and analyzer were arranged in a $(+ - + -, + - + -)$ parallel Nicol geometry, all of the X-rays with an energy spread of 1.5 eV reflected by the polarizer also satisfy the Bragg condition of the analyzer. X-ray intensities upstream and downstream of the phase-retarder system, which consisted of four diamond crystals, were monitored with ionization chambers IC_1 and IC_2.

The phase retarders PR_1, PR_2, PR_3 and PR_4 were (100)-oriented diamond crystals with diameters of about 5 mm and with thicknesses of 318, 314, 301 and 313 μm, respectively. About 13% of the incident X-rays were transmitted through the four diamond crystals. Each diamond crystal was mounted on a goniometer whose axis was adjusted to be perpendicular to the direction of the incident X-rays and to be inclined by 45 or $-45°$ with respect to the polarized direction of the incident X-rays. Each goniometer was driven with a rate of $0.09''$/pulse. The X-ray intensity reflected by each phase-retarder crystal was monitored with a PIN photodiode. According to Hirano et al. (1995) and Hirano (1996), a phase shift given by the transmission-type X-ray phase retarder is approximately proportional to $t/\Delta\theta$. Here, t is not a time but a crystal thickness of the phase retarder and $\Delta\theta$ is an angular deviation of the incident X-rays from the Bragg condition. Therefore, lengths of phase-shift-gradient vectors drawn in Figs. 4, 5 and 6 are approximately proportional to differentiation of phase

research papers

Table 1
Experimental results shown in Figs. 8 and 9 were obtained under the following conditions: $|\Delta\theta_4|^{(max)}$ and $|\Delta\theta_4|^{(min)}$: maximum and minimum absolute values of measured ranges of $\Delta\theta_4$, where $\Delta\theta_4$ is the angular deviation from the Bragg condition of phase retarder PR_4 in arcsec $\Delta\theta_4^{(step)}$: angular step in $''$; Mt: measuring time in s.

	$|\Delta\theta_4|^{(max)}$	$|\Delta\theta_4|^{(min)}$	$\Delta\theta_4^{(step)}$	Mt
Range 1	900.00	180.00	18.00	1.0
Range 2	171.00	99.00	9.00	1.0
Range 3	90.00	63.00	4.50	2.0
Range 4	58.50	49.68	0.18	4.0
Range 5	49.50	27.00	4.50	1.0
Range 6	25.20	0.00	1.80	1.0

shift, that is $t_n/\Delta\theta_n^2$. Here, t_n and $\Delta\theta_n$ are a thickness and an angular deviation from the Bragg condition, respectively, of phase retarder PR_n. Consequently, a condition that $\sum_{n=1}^4 \text{grad}(\Delta\phi_n^{(L)}) = 0$ can be realized in the case of Fig. 7(c) when the four phase retarders are rotated so as to satisfy the following condition:

$$\frac{t_1}{\Delta\theta_1^2} = \frac{t_2}{\Delta\theta_2^2} = \frac{t_3}{\Delta\theta_3^2} = \frac{t_4}{\Delta\theta_4^2}. \tag{10}$$

In order to compare the degrees of vertical-linear polarization available with the arrangements in Figs. 7(a), 7(b) and 7(c), residual components of horizontal-linear polarization of transmitted X-rays were measured with a germanium solid-state detector (SSD) by rotating the four phase-retarder crystals simultaneously. In each case in Figs 7(a), 7(b) and 7(c), PR_n ($n \in \{1, 2, 3, 4\}$) were controlled so as to satisfy the condition of (10). Here, all four crystals were rotated from a lower-angle to a higher-angle side of the Bragg condition in the cases of Figs. 7(a) and 7(b). On the other hand, in the case of Fig. 7(c), PR_2 and PR_4 were rotated from the low-angle side to the high-angle side of the Bragg condition, but PR_1 and PR_3 were rotated reversely. This is due to the reversal of sign of the phase shift between odd-numbered- and even-numbered-quadrant phase retarders as described by (8) and (9). The angular ranges and steps with which the diamond crystals were rotated and measuring times are summarized in Table 1.

5. Results and discussion

Figs. 8(a), 8(b) and 8(c) show experimental results with the setups shown in Figs. 7(a), 7(b) and 7(c), respectively. In order to make a fair comparison among the three kinds of phase-retarder systems, the total thickness of the diamond crystals should be kept the same. If the comparison were to be made with different thicknesses, it would impose more severe condition on a phase retarder with a thinner thickness because the phase retarder has to work more in the vicinity of the Bragg condition where the phase-shift gradient is steeper. The abscissas are angular deviations of one of the phase retarders, $\Delta\theta_4$. The right ordinates in arbitrary linear scales are X-ray intensities reflected by each of the four phase retarders. The left ordinates in logarithmic scales are $I_h(\Delta\theta_4)/[I_v(\Delta\theta_4) + I_h(\Delta\theta_4)]$, where $I_v(\Delta\theta_4)$ and $I_h(\Delta\theta_4)$ are

vertical and horizontal polarization components of X-ray intensity incident on the analyzer crystal, respectively. $I_h(\Delta\theta_4)/[I_v(\Delta\theta_4) + I_h(\Delta\theta_4)]$ were calculated from X-ray intensities measured with IC_2 and SSD based on the procedure described in our previous paper (Okitsu et al., 2001). Our aim is to estimate precisely the decrement of degree of vertical polarization from unity, $2I_h(\Delta\theta_4)/[I_v(\Delta\theta_4) + I_h(\Delta\theta_4)]$. $I_h(\Delta\theta_4)$ [photons s^{-1}] can be measured by counting photons with SSD in Fig. 7. Although the value of the current $I_{total}(\Delta\theta_4)$ [A] is proportional to $I_v(\Delta\theta_4) + I_v(\Delta\theta_4)$ [photons s^{-1}], $I_v(\Delta\theta_4)$ cannot directly be measured. $I_v(\Delta\theta_4) + I_h(\Delta\theta_4)$ is given by

$$I_v(\Delta\theta_4) + I_h(\Delta\theta_4) = cI_{total}(\Delta\theta_4). \tag{11}$$

Therefore,

$$c = \frac{I_v(\Delta\theta_4) + I_h(\Delta\theta_4)}{I_{total}(\Delta\theta_4)}. \tag{12}$$

Here, c is a proportional constant depending on the detection efficiency of ionization chamber IC_2 in Fig. 7. Therefore, $I_h(\Delta\theta_4)/[I_v(\Delta\theta_4) + I_h(\Delta\theta_4)]$ is given by
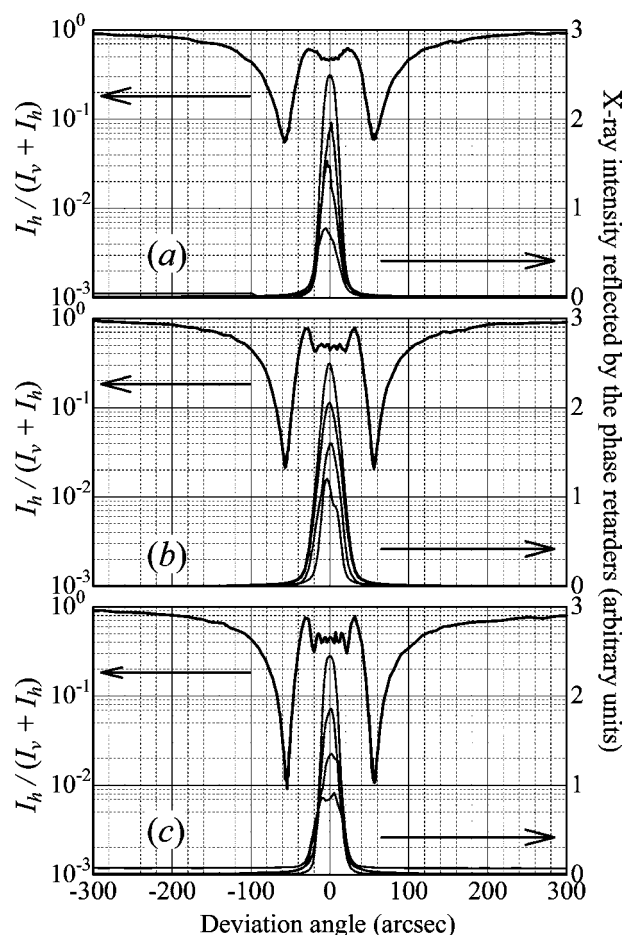
Figure 8
Rate of a residual horizontally polarized component after the conversion from horizontally polarized X-rays by the phase-retarder systems. (a), (b) and (c) are obtained under the geometries shown in Figs. 7(a), 7(b) and 7(c), respectively. Photon energy: 7709 eV; energy spread: 1.5 eV; angular divergence: 45''. The abscissas are values of $\Delta\theta_4$.

$$\frac{I_h(\Delta\theta_4)}{I_v(\Delta\theta_4) + I_h(\Delta\theta_4)} = \frac{I_h(\Delta\theta_4)}{cI_{\text{total}}(\Delta\theta_4)}. \tag{13}$$

Since (11), (12) and (13) are satisfied with the same constant value c at each value of $\Delta\theta_4$, the value of c has to be determined with a high precision in order to calculate $I_h(\Delta\theta_4)/[I_v(\Delta\theta_4) + I_h(\Delta\theta_4)]$ precisely. On the other hand, ellipticity $R(\Delta\theta_4)$ of elliptically polarized X-rays produced by the experimental setup as shown in Fig. 5 is given as follows (Okitsu, Oguchi *et al.*, 1998; Okitsu, Ueji, Oguchi, Hasegawa *et al.*, 1998, Okitsu, Ueji, Oguchi, Maruyama *et al.*, 1998):

$$R(\Delta\theta_4) = \tan\left(\frac{\sum_{n=1}^{4} \Delta\phi_n^{(L)}(\Delta\theta_n)}{2}\right). \tag{14}$$

The $I_v(\Delta\theta_4) : I_h(\Delta\theta_4)$ ratio is given by

$$\frac{I_v(\Delta\theta_4)}{I_h(\Delta\theta_4)} = R^2(\Delta\theta_4). \tag{15}$$

By substituting (15) for (12), we obtain

$$c = \frac{I_h(\Delta\theta_4)[1 + R^2(\Delta\theta_4)]}{I_{\text{total}}(\Delta\theta_4)}. \tag{16}$$

We have to determine c with R as small as possible. According to Hirano *et al.* (1995) and Hirano (1996), $\Delta\phi_n(\Delta\theta_n)$ is approximately proportional to $t_n/\Delta\theta_n$. Since $R(\Delta\theta_4)$ is given by (14), the value of $|R(\Delta\theta_4)|$ is small when $|\Delta\theta_n|$ are large values. From calculations based on the dynamical diffraction theory, a value of $R^2(-900'')$ was calculated to be 0.026. By substituting the value of $R^2(-900'')$ into (16) and substituting (16) into (13), we obtain

$$\frac{I_h(\Delta\theta_4)}{I_v(\Delta\theta_4) + I_h(\Delta\theta_4)} = \frac{I_{\text{total}}(-900'')I_h(\Delta\theta_4)}{1.026\ I_h(-900'')I_{\text{total}}(\Delta\theta_4)}. \tag{17}$$

Two dips are observed at $\Delta\theta_4 \simeq \pm 60''$ in Figs. 8(*a*), 8(*b*) and 8(*c*). This indicates that maximum degrees of vertical-linear polarization were created there. These values at left and right dips, $P_v^{(L.\max)}$ and $P_v^{(R.\max)}$ in Fig. 8 can be calculated by using (1) and (17). These values were 0.880–0.889, 0.958 and 0.979–0.982 in the cases of Figs. 8(*a*), 8(*b*) and 8(*c*), respectively. It is clear that two-quadrant geometry corresponding to the double phase retarders (Okitsu *et al.*, 2001) creates higher degrees of vertical polarization than one-quadrant geometry corresponding to a single phase retarder. This is due to the effect of compensation for off-axis aberration. In addition, the four-quadrant geometry gives higher degrees of vertical-linear polarization than two-quadrant geometry. This means that not only the off-axis aberration but also the chromatic aberration are compensated with the four-quadrant geometry. It is noteworthy that fine oscillatory profiles that reveal rapid changes of phase shift are found between the dips in the vicinity of the Bragg condition, in the cases of Figs. 8(*b*) and 8(*c*). Such oscillatory profiles are blurred and not found due to the aberrations in the case of Fig. 8(*a*). The oscillatory profiles can be more clearly observed in the case of Fig. 8(*c*) than in the case of Fig. 8(*b*), resulting from the effect of compensation for the chromatic aberration.

Here, we will discuss the residual aberration of the four-quadrant phase retarder. The experimental result in Fig. 9 was obtained with the four-quadrant phase-retarder system when the energy spread and the angular divergence of the incident X-rays were decreased from 1.5 to 0.5 eV and from 45 to 20″, respectively. In the experiment, the degree of vertical-linear polarization had increased from 0.98 to 0.994. This increase in the degree of vertical-linear polarization means that there still remain off-axis and chromatic aberrations even with the four-quadrant phase retarder. This residual aberration is attributed to second-order differentiation terms of the phase shift given by the phase-retarder system. This result reveals that beam collimation and suppressed energy spread of incident X-rays are still effective to obtain a higher degree of polarization with the four-quadrant X-ray phase-retarder system.

We have successfully measured X-ray natural-linear-dichroism (XNLD) spectra with a Co single-crystal foil (Sato, Okitsu *et al.*, 2000; Sato, Ueji *et al.*, 2000) by using a linear-polarization switching technique with the four-quadrant phase-retarder system. In the linear-polarization switching technique, vertical- and horizontal-linear polarizations can be alternated in 1–2 s. The measured degree of horizontal-linear polarization has reached 0.9999. Here, zero phase shift was achieved by canceling out the phase shifts by odd-numbered-quadrant phase retarders and by even-numbered-quadrant phase retarders. For example, we can use angular regions indicated by circles of the left-hand part in Fig. 6 coupled with regions indicated by squares of the left-hand part to generate a horizontal-linear polarization. Neither removal of the phase retarders from the X-ray beam path nor rotation of the phase retarder far from the Bragg condition is required, which prevents quick polarization switching. This is another advantage of the multiple (double and/or four-quadrant) phase-retarder system (Okitsu *et al.*, 2001).
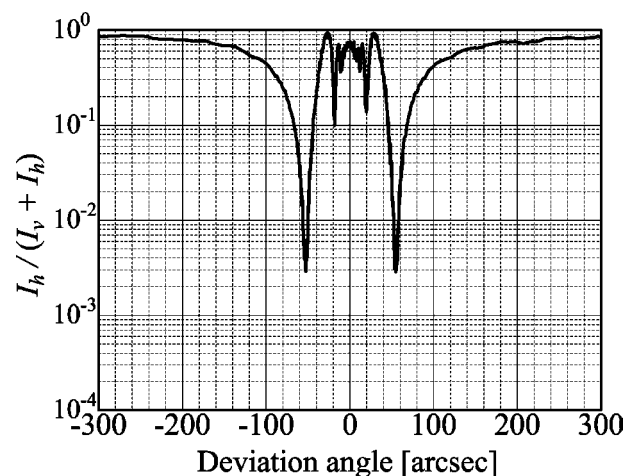
Figure 9
Rate of a residual horizontally polarized component after the conversion from horizontally polarized X-rays by the four-quadrant phase-retarder system. Photon energy: 7709 eV; energy spread: 0.5 eV; angular divergence: 20″. The abscissa is the value of $\Delta\theta_4$.

6. Conclusions

We have developed a four-quadrant X-ray phase-retarder system that can compensate for both off-axis and chromatic aberrations and its advantage over the single and double phase-retarder systems has been confirmed experimentally. Under a condition of 7709 eV photon energy, 1.5 eV energy spread and 45″ angular divergence (FWHM) of incident X-rays, the four-quadrant X-ray phase-retarder system created 0.98 degree of vertical-linear polarization from horizontal-linear polarization. This value was favorably compared with 0.89 and 0.96 degree, which were obtained by the single and double phase-retarder systems, respectively, which have the same total thicknesses of the phase retarders. Since a conversion from horizontal to vertical polarization requires a phase shift as large as π (180°), the present estimation was performed under the most severe condition regarding phase-shift homogeneity of the transmission-type phase retarder. For example, when left-handed- and right-handed-circular polarizations are needed, that is when a phase shift of $\pm\pi/2$ is required, a better phase-shift homogeneity is available with the four-quadrant phase-retarder system. Thus, this system can provide high degrees of X-ray polarization for experiments which require polarization switching.

References

Alagna, L., Prosperi, T., Turchini, S., Goulon, J., Rogalev, A., Goulon-Ginet, C., Natoli, C. R., Peacock, R. D. & Stewart, B. (1998). *Phys. Rev. Lett.* **80**, 4799–4802.

Annaka, S. (1982). *J. Phys. Soc. Jpn*, **51**, 1927–1931.

Annaka, S., Suzuki, T. & Onoue, K. (1980). *Acta Cryst.* **A36**, 151–152.

DuMond, J. W. M. (1937). *Phys. Rev.* **52**, 872–883.

Giles, C., Malgrange, C., Goulon, J., Bergevin, F., Vettier, C., Fontaine, A., Dartyge, E. & Pizzini, S. (1994). *Nucl. Instrum. Methods*, A**349**, 622–625.

Giles, C., Malgrange, C., Goulon, J., Vettier, C., Dartyge, E., Fontaine, A., Giorgetti, C. & Pizzini, S. (1994). *J. Appl. Cryst.* **27**, 232–240.

Giles, C., Vettier, C., Bergevin, F., Malgrange, C., Grübel, G. & Grossi, F. (1995). *Rev. Sci. Instrum.* **66**, 1518–1521.

Golovchenko, J. A., Kincaid, B. M., Lvesque, R. A., Meixner, A. E. & Kaplan, D. R. (1986). *Phys. Rev. Lett.* **57**, 202–205.

Goulon, J., Goulon-Ginet, C., Rogalev, A., Gotte, V., Malgrange, C., Brouder, C. & Natoli, C. R. (1998). *J. Chem. Phys.* **108**, 6394–6403.

Hart, M. (1978). *Philos. Mag.* B**38**, 41–56.

Hart, M. & Rodrigues, A. R. D. (1979). *Philos. Mag.* B**40**, 149–157.

Hirano, K. (1996). *J. Crystallogr. Soc. Jpn*, **38**, 221–228. (In Japanese.)

Hirano, K., Ishikawa, T. & Kikuta, S. (1993). *Nucl. Instrum. Methods Phys. Res. A*, **336**, 343–353.

Hirano, K., Ishikawa, T. & Kikuta, S. (1995). *Rev. Sci. Instrum.* **66**, 1604–1609.

Hirano, K., Ishikawa, T., Koreeda, S., Fuchigami, K., Kanzaki, K. & Kikuta, S. (1992). *Jpn. J. Appl. Phys.* **31**, L1209–L1211.

Hirano, K., Izumi, K., Ishikawa, T., Annaka, S. & Kikuta, S. (1991). *Jpn. J. Appl. Phys.* **30**, L407-L410.

Ishikawa, T., Hirano, K., Kanzaki, K. & Kikuta, S. (1992). *Rev. Sci. Instrum.* **63**, 1098–1103.

Ishikawa, T., Hirano, K. & Kikuta, S. (1991). *J. Appl. Cryst.* **24**, 982–986.

Mills, D. M. (1987). *Phys. Rev. B*, **36**, 6178–6181.

Okitsu, K., Oguchi, T., Maruyama, H. & Amemiya, Y. (1998). *J. Synchrotron Rad.* **5**, 995–997.

Okitsu, K., Ueji, Y., Oguchi, T., Hasegawa, Y., Ohashi, Y. & Amemiya, Y. (1998). *J. Synchrotron Rad.* **5**, 1055–1057.

Okitsu, K., Ueji, Y., Oguchi, T., Maruyama, H., Hasegawa, Y. & Amemiya, Y. (1998). *J. Crystallogr. Soc. Jpn*, **40**, 341–354. (In Japanese.)

Okitsu, K., Ueji, Y., Sato, K. & Amemiya, Y. (2001). *J. Synchrotron Rad.* **8**, 33–37.

Sato, K., Okitsu, K., Ueji, Y., Matsushita, T. & Amemiya, Y. (2000). *J. Synchrotron Rad.* **7**, 368–373.

Sato, K., Ueji, Y., Okitsu, K., Hasegawa, Y., Matsushita, T. & Amemiya, Y. (2000). *J. Jpn. Soc. Synchrotron Rad. Res.* **13**, 304–312. (In Japanese.)

Sato, K., Ueji, Y., Okitsu, K., Matsushita, T. & Amemiya, Y. (2001). *J. Synchrotron Rad.* **8**, 1021–1026.

Sato, K., Ueji, Y., Okitsu, K., Matsushita, T., Saito, J., Takayama, T. & Amemiya, Y. (2001*a*). *J. Magn. Soc. Jpn*, **25**, 206–209.

Sato, K., Ueji, Y., Okitsu, K., Matsushita, T., Saito, J., Takayama, T. & Amemiya, Y. (2001*b*). *Phys. Rev. B*, **64**. Submitted.

Skalicky, P. & Malgrange, C. (1972). *Acta Cryst.* **A28**, 501–507.

Ueji, Y., Okitsu, K., Sato, K. & Amemiya, Y. (2000). *J. Jpn. Soc. Synchrotron Rad. Res.* **13**, 48–56. (In Japanese.)